Elsevier Editorial System(tm) for Wear
Manuscript Draft

Manuscript Number:

Title: Influence of pre-existing martensite on the wear resistance of metastable austenitic stainless steels

Article Type: Full-Length Article

Keywords: Keywords: metastable austenitic stainless steels, martensite, sliding wear, advanced characterization techniques.

Corresponding Author: Dr. Gemma Fargas,

Corresponding Author's Institution: CIEFMA-UPC

First Author: Gemma Fargas

Order of Authors: Gemma Fargas; JOAN JOSEP ROA; ANTONIO MATEO

Abstract: The effect of pre-existing martensite on the sliding wear behaviour of a commercial metastable austenitic stainless steel was investigated. Two different steel conditions were considered: annealed (with a fully austenitic microstructure) and cold rolled, consisting of mixtures of austenite and martensite. Wear tests were carried out using ball on disc technique at constant velocity and different sliding distances. Correlation between microstructure and wear mechanisms was performed by X-ray diffraction, electron back-scattered diffraction and focus ion beam. Results show that wear resistance decrease at increasing the amount of pre-existing martensite. In this sense, the strain-induced martensite developed at higher degree for cold rolled samples which strengths the surface and consequently reduces plowing wear mechanism, typical of ductile abrasive wear. The detailed analysis of the wear track demonstrated the formation of ultrafine-grains layer just below the surface not only for annealed but also for cold rolled steel conditions. For both cases, the main wear mechanism developed for the studied sliding distances was tribocorrosion.

WEAR

Confirmation of Authorship

Please save a copy of this MS Word file, complete and upload as the "Confirmation of Authorship" file.

As corresponding author, I Gemma Fargas, hereby confirm on behalf of all authors that:

1) The authors have obtained the necessary authority for publication.
2) The paper has not been published previously, that it is not under consideration for publication elsewhere, and that if accepted it will not be published elsewhere in the same form, in English or in any other language, without the written consent of the publisher.
3) The paper does not contain material which has been published previously, by the current authors or by others, of which the source is not explicitly cited in the paper.

Upon acceptance of an article by the journal, the author(s) will be asked to transfer the copyright of the article to the publisher. This transfer will ensure the widest possible dissemination of information.

***Novelty Statement**

TRIP steels present a metastable austenitic phase which transforms to martensite due to plastic deformation, either during forming or under service conditions. Numerous investigations have shown that pre-existing martensite enhance mechanical properties.

The present work was performed with the purpose of investigating the wear behavior of metastable austenitic stainless steels. Some research on this topic can be found in the literature, where several studies demonstrated that strain-induced martensite was formed during dry sliding tests. However, no information exists about the influence of pre-existing martensite. In this sense, four different steel conditions were selected: annealed, with fully austenitic microstructure, and cold rolled up to 10, 20 and 40 % thickness reduction, with a biphasic microstructure composed by austenite and martensite phases. In order to correlate microstructural characteristics and wear mechanisms in deteail, several techniques such as X-Ray diffraction, Scanning Electron Microscopy (SEM), EBSD, and Focus Ion Beam (FIB), have been used.

Influence of pre-existing martensite on the wear resistance of metastable austenitic stainless steels

G. Fargas *, J. J. Roa, A. Mateo

CIEFMA - Departament de Ciència dels Materials i Enginyeria Metal·lúrgica. Universitat Politècnica de Catalunya. Avda. Diagonal 647, 08028, Barcelona (Spain)

* Corresponding author, e-mail: gemma.fargas@upc.edu

Abstract

The effect of pre-existing martensite on the sliding wear behaviour of a commercial metastable austenitic stainless steel was investigated. Two different steel conditions were considered: annealed (with a fully austenitic microstructure) and cold rolled, consisting of mixtures of austenite and martensite. Wear tests were carried out using ball on disc technique at constant velocity and different sliding distances. Correlation between microstructure and wear mechanisms was performed by X-ray diffraction, electron back-scattered diffraction and focus ion beam. Results show that wear resistance decrease at increasing the amount of pre-existing martensite. In this sense, the strain-induced martensite developed at higher degree for cold rolled samples which strengths the surface and consequently reduces plowing wear mechanism, typical of ductile abrasive wear. The detailed analysis of the wear track demonstrated the formation of ultrafine-grains layer just below the surface not only for annealed but also for cold rolled steel conditions. For both cases, the main wear mechanism developed for the studied sliding distances was tribocorrosion.

Keywords: metastable austenitic stainless steels, martensite, sliding wear, advanced characterization techniques.

1. Introduction

Recent developments of steel manufacturers have led to the commercialization of multiphase TRIP (Transformation Induced Plasticity) steels in order to produce lightweight vehicles that reduce fuel consumption and also contaminant emissions [1]. TRIP steels present a metastable austenitic phase which transforms to martensite due to plastic deformation, either during forming or under service conditions [2]. The

martensite induced by forming processes is called pre-existing martensite. This phase transformation acts as a reinforcing mechanisms which make those steels ideal materials to replace the conventional steel grades due to their excellent combination of formability, crash-absorbing capability, and also good corrosion resistance [3].

Two types of martensite may form in austenitic stainless steels: ε and α'. ε-martensite has a hcp crystallographic structure, while α' has a bcc one [4]. The typical transformation sequence can be summarized as: γ-ε-α', where the $\gamma \rightarrow \varepsilon$ transformation has been proposed for austenitic stainless steels deformed under tension, as well as by rolling [5,6]. On the other hand, the direct transformation of austenite to α'-martensite ($\gamma \rightarrow \alpha'$) has been observed too, as found elsewhere [7]. The amount of induced martensite depends on processing parameters, such as stress rate, temperature and rate of deformation [8], as well as composition [9,10,11]. Furthermore, plastic deformation of austenite creates the proper defect structure which acts as nucleation site for martensite formation [12]. The dislocation arrangements in the deformed austenite are strongly dependent upon the alloy chemistry, stress, strain, stress triaxiality, strain rate, initial micro-textures, slip systems, temperature of deformation and the extent of deformation-induced phase transformation [13].

Numerous investigations have shown that pre-existing martensite enhance mechanical properties [14,15,16,17,18,19,20]. In this sense, the higher the percentage of martensite, the higher the values of yield stress, ultimate strength, and hardness. Regarding fatigue response, there are extensive studies in the literature which demonstrated that metastable stainless steels display different behaviors depending on the testing conditions [21,22,23,24,25]. The presence of martensite is known to be harmful in the low cycle fatigue regime (i.e. under strain-control), while a small amount of martensite can be beneficial in the high cycle fatigue regime.

The present work was performed with the purpose of investigating the wear behavior of metastable austenitic stainless steels. Some research on this topic can be found in the literature, where several studies demonstrated that strain-induced martensite was formed during dry sliding tests [26,27,28,29,30]. However, no information exists about the influence of pre-existing martensite. In this sense, four different steel conditions were selected: annealed, with fully austenitic microstructure, and cold rolled up to 10, 20 and 40 % thickness reduction, with a biphasic microstructure composed by austenite and martensite phases. In order to correlate microstructural characteristics and wear

mechanisms, several techniques such as X-Ray diffraction, Scanning Electron Microscopy (SEM), EBSD, and Focus Ion Beam (FIB), have been used.

2. Experimental process

The experimental material was a commercial AISI 301 LN austenitic stainless steel (corresponding to standard EN 1.4318) provided by OCAS NV, Arcelor-Mittal R&D Industry Gent (Belgium). Its chemical composition was (in wt. %): Fe-0.03C-17.36Cr-7.18Ni-1.68Mn- 0.23Mo-0.55Si-0.14N.

Sheets of 1.5 mm in thickness were supplied in four different conditions. The condition named AR corresponded to cold rolling, annealing and pickling. Its microstructure showed equiaxial austenitic grains (average grain size of 11.7 ± 4.1 μm), randomly oriented, with twins created during annealing treatment. The three other conditions had an additional last cold rolling step performed to achieve different percentages of pre-existing martensite. The thickness reductions were 10, 20 and 40 %, that will be referred in the present work as 10CR, 20CR and 40 CR, respectively. The amount of martensite and the corresponding mechanical properties of the four steel conditions are found elsewhere [20] and also summarized in Table 1.

Table 1. Martensite content and mechanical properties for the studied steel conditions.

	% martensite	σ_{YS} (MPa)	σ_{UTS} (MPa)	%A	HV0.1
AR	<3	360±10	902±15	42±1	246±8
10CR	9±3	650±14	967±18	38±3	290±10
20CR	28±7	926±17	1113±17	30±3	400±5
40CR	38±5	1148±16	1173±19	22±2	440±8

For wear tests, specimens were polished up to roughness values lower than R_a = 0.7 μm, following the guidelines of ASTM G99 standard [31]. Sliding wear tests were performed using ball on disc technique in a tribometer TRM-1000 of Wazau GmbH. The ball used was of tungsten carbide, of 10 mm diameter and a hardness of 1600 HV10. Dry sliding wear tests were carried out at a constant load of 10 N and a mean linear velocity of 0.048 m/s for all sliding distances: 100, 200, 300, 500 and 1000 m.

Before and after each wear test, balls and specimens were ultrasonically cleaned for 15 minutes, dried with a pure air and weighted by an electronic balance having a resolution of ± 0.1 mg. The wear volume was determined using weight loss measurements and wear track profile method. In the latter case, wear volume was determined by measuring the cross-section area of the material displaced at the edges at eight equidistant positions along the wear track.

The amount of induced-martensite as a consequence of the deformation introduced by the ball in contact with surface during wear tests was achieved by X-Ray diffraction. The phase components were identified with Copper radiation. Determination of martensite content was carried out by the method corresponding to reference intensity ratio (RIR), according to ASTM E975-03 [32]. This method allows determining the mass fractions of austenite and martensite by using equation (1):

$$\frac{X_{\alpha'}}{X_{\gamma}} = \frac{RIR_{\gamma}}{RIR_{\alpha'}} \times \frac{I_{\alpha',\, observed}}{I_{\gamma,\, observed}} \times \frac{I_{\gamma,\, reference}}{I_{\alpha',\, reference}} \qquad (1)$$

where X_{α} and X_{γ} are the mass fractions of α'-martensite and γ-austenite, respectively; RIR_{γ} and RIR_{α} are their respective reference intensity ratios; $I_{observed}$ and $I_{reference}$ are the observed and the reference intensities [32].

EBSD scans were performed in a JSM-7001F field emission scanning electron microscope (FESEM) equipped with Channel 5 system (HKL Technology), operating at 20 kV with specimens tilted 70 degrees.

Hardness profiles were performed on cross-section specimens in order to elucidate the strengthening of austenite in subsurface due to wear tests. Vickers hardness measurements at 0.1 kg load were carried on at the deepest zone of the wear track until the center of the sheet (0.8 mm) or at least to a constant hardness value. An array of 4 columns of indents spaced 100 μm was performed in order to get statistical signification.

The deformed microstructure on the subsurface was analyzed by a dual FIB/FESEM. A thin platinum layer was deposited on the sample prior to FIB machining in order to minimize ion beam damage. A Ga^{+} ion source was used to mill the surface at a voltage of 5 kV. The final polishing of the cross-sections was made at 500 pA.

Wear tracks and the induced surface damage were examined by optical microscopy (OM), confocal laser scanning microscopy (CLSM), scanning electron microscopy (SEM) and energy-dispersive X-ray spectroscopy (EDX) to elucidate the wear mechanisms developed for each studied steel condition.

3.- Results and discussion

The wear maps representing the wear volume as a function of the sliding distance are given in Figure 1. A strong influence of the amount of pre-existing martensite is clearly observed. In this regard, the higher the cold rolled thickness reduction, i.e. larger initial content of martensite, specimens displayed less resistance to wear. After 1000 m of sliding distance, the wear volume of 40CR specimens was more than three times higher than for the annealed condition.

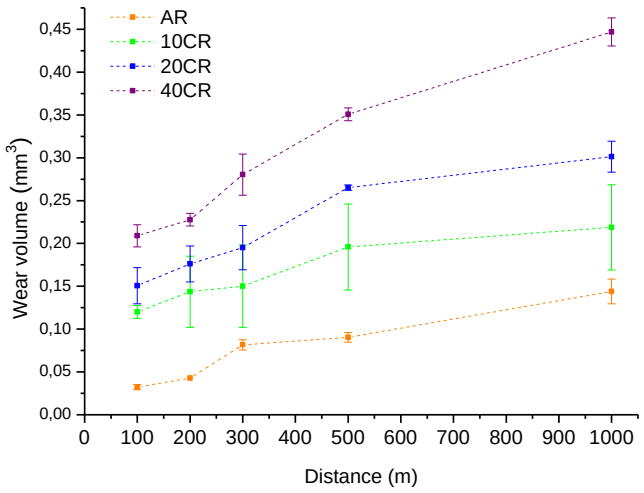

Figure 1. Wear volume for all the studied steel conditions as a function of sliding distance.

As it can be seen in Figure 2, wear rate gradually diminishes when increasing sliding distance. Differences between annealed and cold rolled conditions were especially relevant for the first 300 m. Even specimens with the smallest percentage of pre-existing martensite (10CR) displayed, for the first 100 m, a wear rate triple than the AR ones.

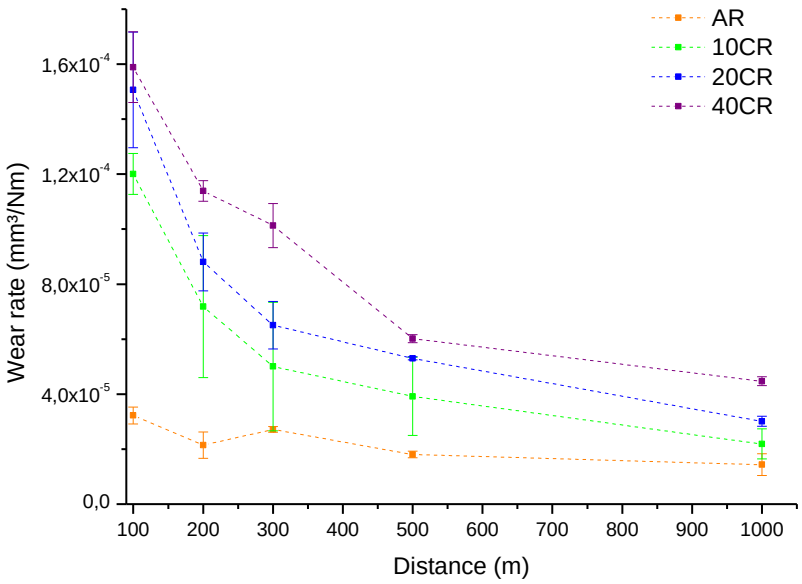

Figure 2. Wear rate for all the studied steel conditions as a function of sliding distances.

X-ray diffraction performed in the wear track revealed peaks of α'-martensite whereas no evidence of ε-martensite was detected. Figure 3 shows that, for all the studied conditions, a strong increase in martensite content took place during the first 100 meters of sliding distance. Afterwards, no further martensite formation was measured neither for AR, in agreement with previous results [27], nor for cold rolled conditions. It is important to highlight that the higher the percentage of pre-existing martensite the more the induced martensite developed during wear tests, as clearly depicted in Figure 4. In this sense, the amount of wear induced martensite became more than 20% for 40CR condition, while for specimens with fully austenitic microstructure was under 10%. These results are in agreement with previous studies which demonstrate that, in austenitic grains deformed by cold working, the presence of microbands and twins provide not only strain hardening but also serve as nucleation sites to promote the formation of strain-induced martensite [33,34,35].

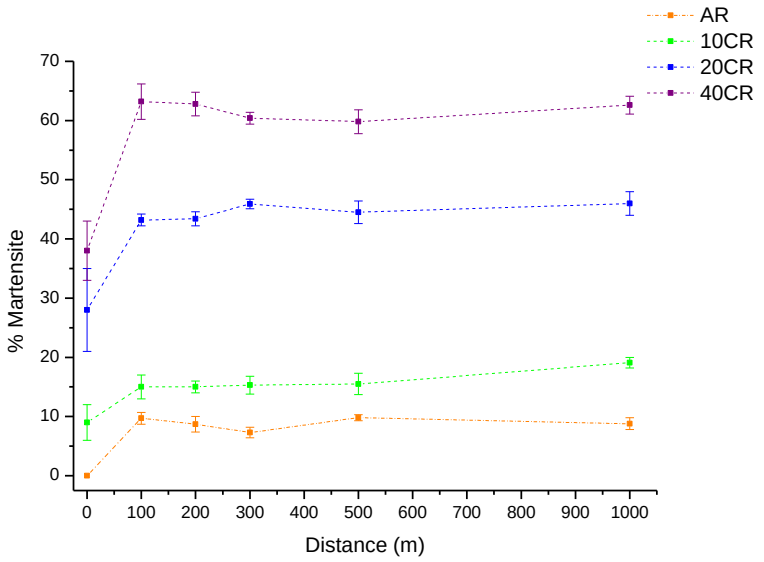

Figure 3. Percentage of martensite as a function of the sliding distance.

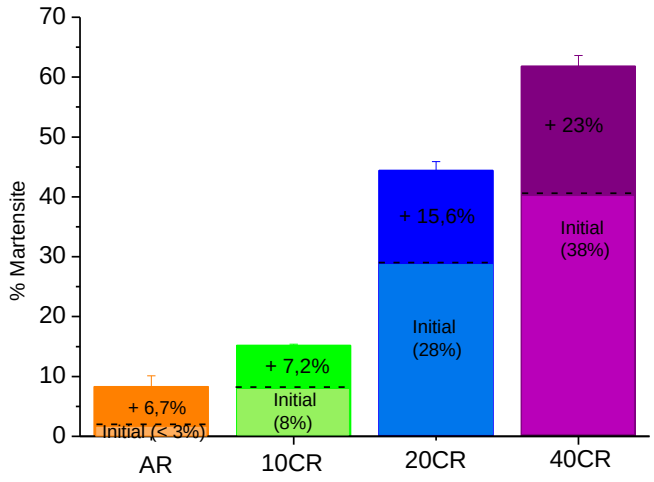

Figure 4. Amount of martensite considering the initial percentage and the strain-induced martensite after 1000 meters of sliding wear test.

The analysis of the track profiles also pointed out that plastic deformation is strongly influenced by the microstructure. The measurement of the abraded material removed from the internal zone of the track to outside, known as plowing wear mechanism, differs depending on the initial percentage of martensite. As it can be observed in Figure 6, plowing volume for AR and 10CR, was from short to large sliding distances higher compared to harder steel conditions (20CR and 40CR), where after 1000m the plowing volume was less than the half measured for softer steel conditions.

Numerous studies have focused on understanding the TRIP effect with regard to plastic deformation. The most widely accepted interpretation [36,37,38,39] is that not only the total amount of induced martensite is significant, but also the rate of transformation for a given plastic strain and at which point it takes place, are the factors that govern the ductility. In this sense, our previous study [20] showed that for cold rolled specimens martensite transformation occurs rapidly in comparison with the same situation for annealed specimens, resulting in abrupt work hardening and, consequently, premature fracture. Considering the foregoing, it seems clear that plowing volume of 20CR and 40CR specimens decreases progressively as increasing sliding distance. For these steels conditions, with a higher presence of pre-existing martensite and also more prone to the formation of strain-induced martensite, plastic deformation becomes more difficult.

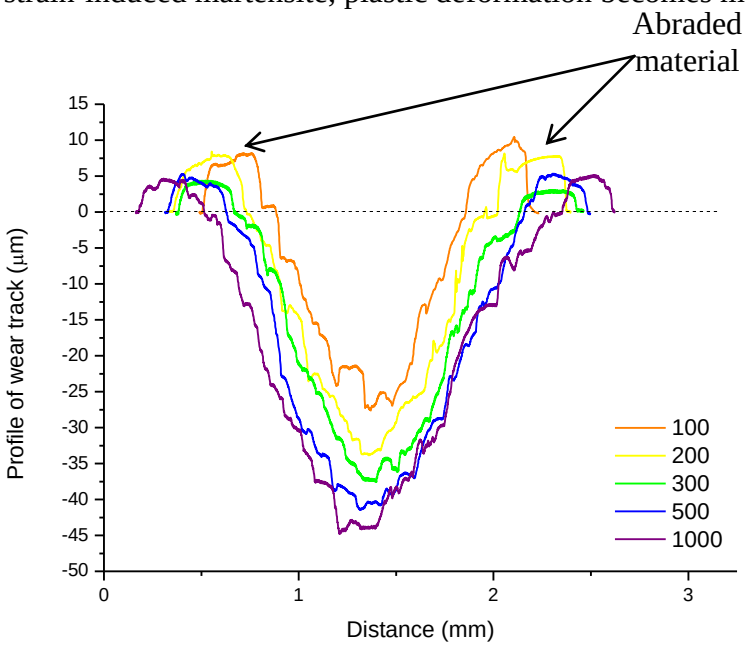

Figure 5. Schematic representation of wear track profile.

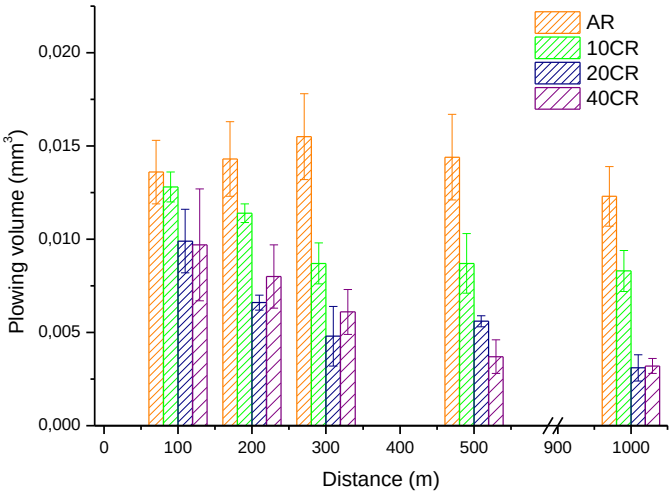

Figure 6. Plowing volumes vs sliding distance for all the studied steel conditions.

A detailed observation of plastic deformation produced in the sub-surface by the continuous contact of the ball during wear tests was performed using FIB for both AR and 40CR conditions. Two regions were studied: the edge and approximately the middle of the wear track, as indicated in Figure 7. In order to reveal the microstructure under those regions, they were exposed to the ion beam during several seconds to produce ion etching. Afterwards, the trenches created were observed by FESEM.

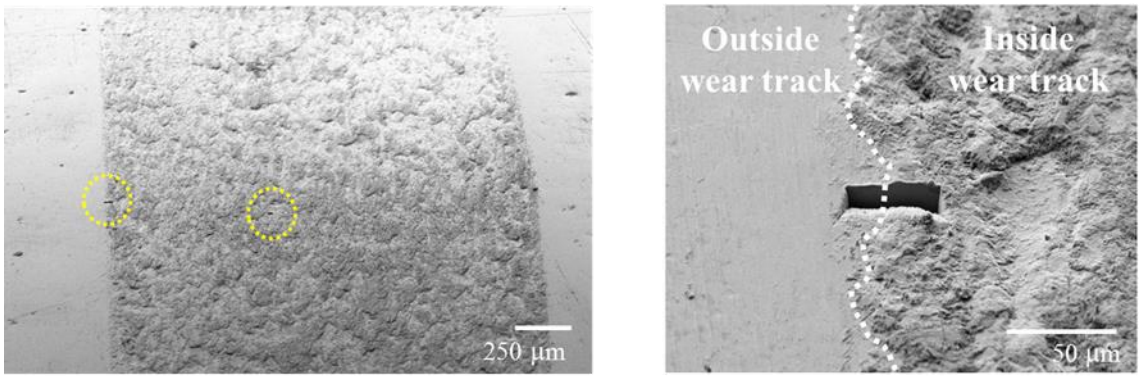

Figure 7. a) Location of the regions studied by FIB: the edge and approximately the middle of the wear track and b) Magnification of a trench performed at the edge of the wear track.

A layer of thickness ranging between 1.0 to 1.5 µm and consisting of ultrafine-grains can be appreciated in FESEM micrographs of AR condition at the edge of wear track, as shown in Figure 8b. Some authors assumed that such layer is related to the surface damage during the sample preparation, mainly by the grinding process and the final polishing step, and no with an amorphization effect induced by the Ga^+ ions [40]. However, in the present work, no sample preparation was carried on specimens before

wear tests. Moreover, this layer only appears at the wear track, whereas there are no indications of ultrafine-grains outside the track, as evidenced in Figure 8d. The formation of this layer due to plastic deformation is in agreement with a previous study carried out by the authors [20] where the cross-section analysis of shot peened specimens of the same here studied stainless steel conditions revealed the formation of an ultrafine-grain layer of 0.5 to 1 μm of thickness. These observations are also corroborated by several studies which describe that severe plastic deformation (SPD) can induce grain size reductions of several orders of magnitude: pure metals can be refined down to maximum 140 nm [41], dispersion alloys to 50 nm [42] and solid solution alloys to 26 nm [43].

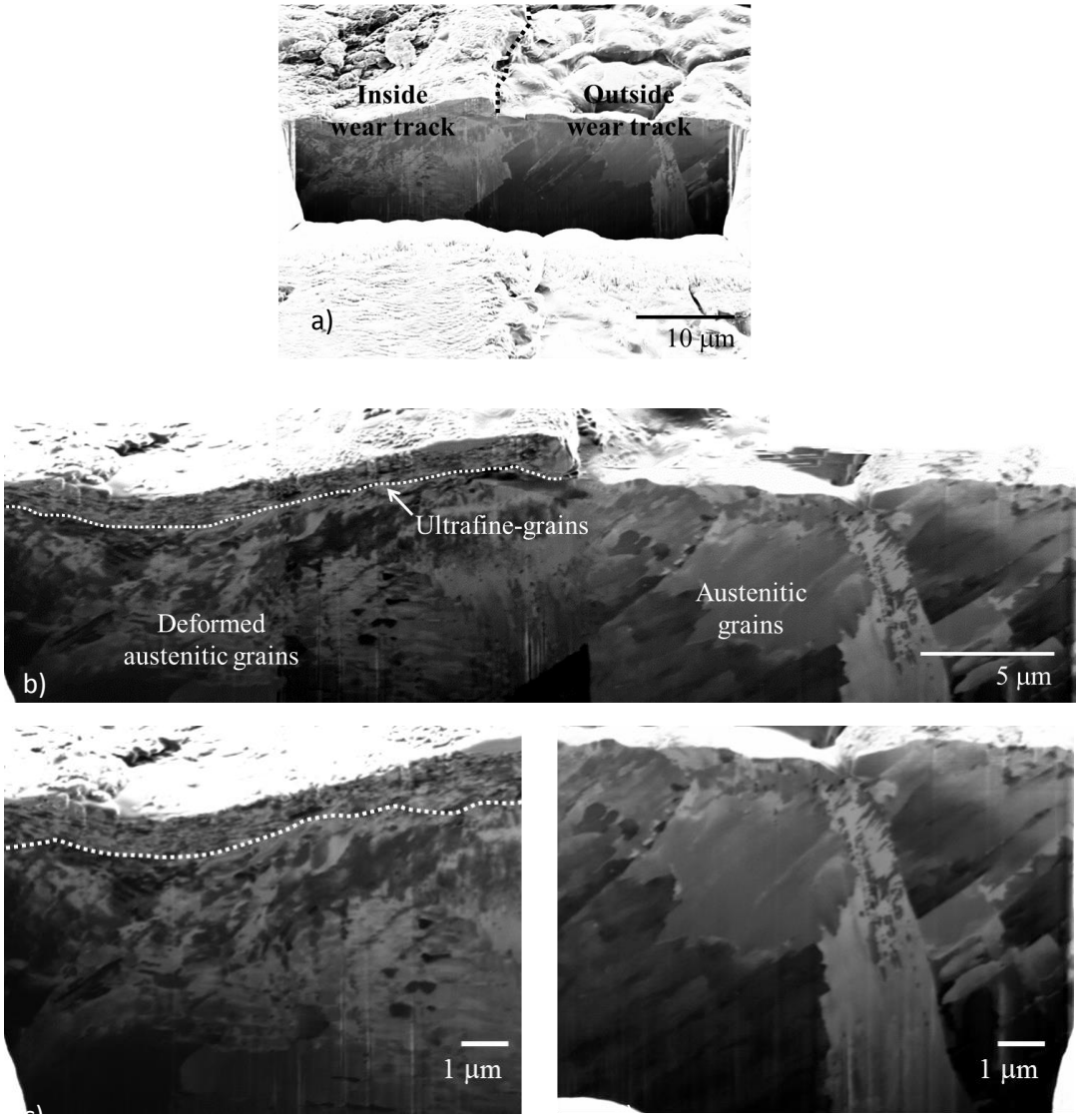

Figure 8. Analysis of the AR subsurface specimens by FIB/FESEM at the edge of the wear track. a) Location of the trench, b) Micrograph of the cross-section, c) Magnification of the zone inside wear track and d) Magnification of the zone outside wear track.

Figure 9 shows that the ultrafine-grains layer was also present in 40CR specimens. Nevertheless, it is important to point out that for this steel condition a thinner layer (< 1μm) appeared outside the wear track (Fig. 9b), probably generated during the final cold rolling step. Furthermore, deformed austenitic grains were visible even outside the wear track, as can be seen in Figure 9d, although in lower degree compared to the austenitic grains just below the wear track (Fig. 9c). In those micrographs, adhered particles were also identified. The presence of these particles reveals that the repeated action of the ball on the surface causes the formation of debris, as a consequence of the material removed from the surface, which later adhere elsewhere in the wear track.

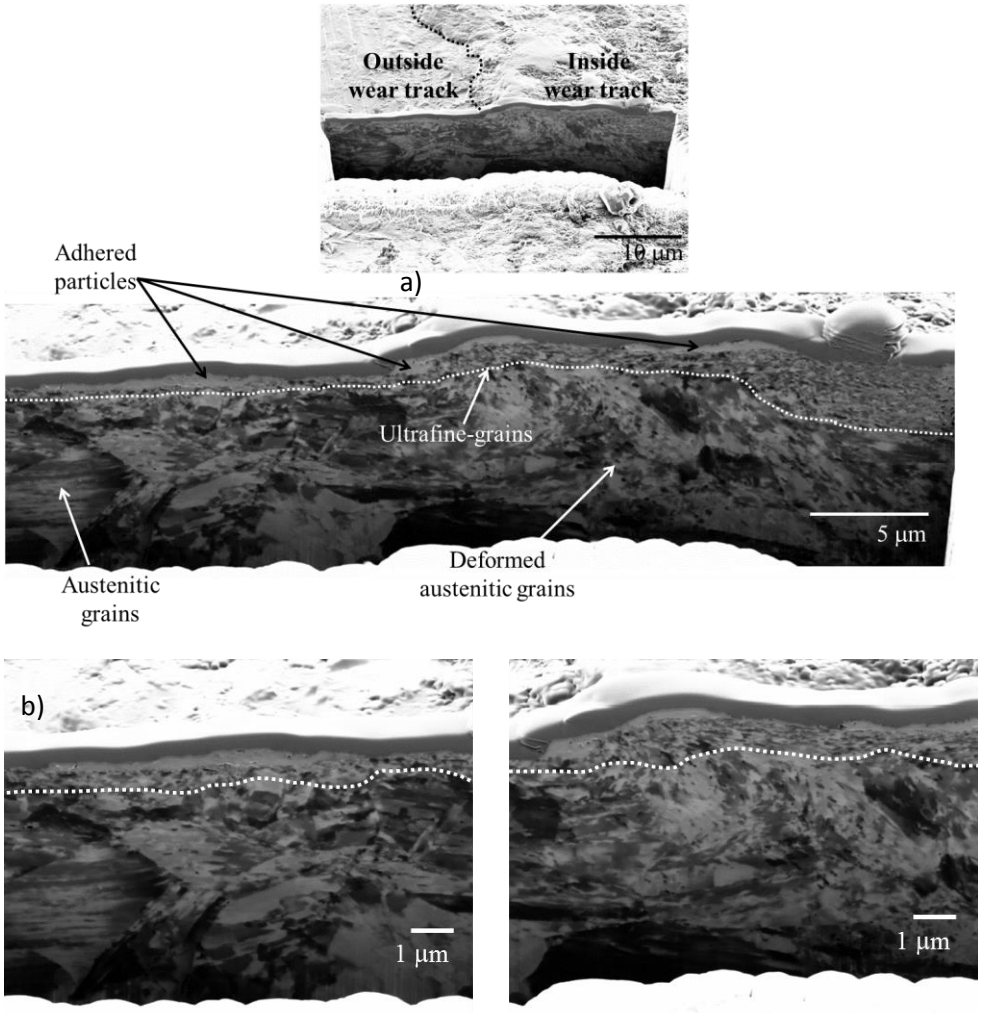

Figure 9. Analysis of the CR subsurface specimens by FIB/FESEM at the edge of the wear track. a) Location of the trench, b) Micrograph of the cross-section, c) Magnification of the zone inside wear track and d) Magnification of the zone outside wear track.

FESEM micrographs acquired for both steel conditions approximately in the middle of the wear track were qualitatively similar to those corresponding to the edge. In both cases the ultrafine-grains layer covered the entire analyzed cross-section, as shown in Figure 10.

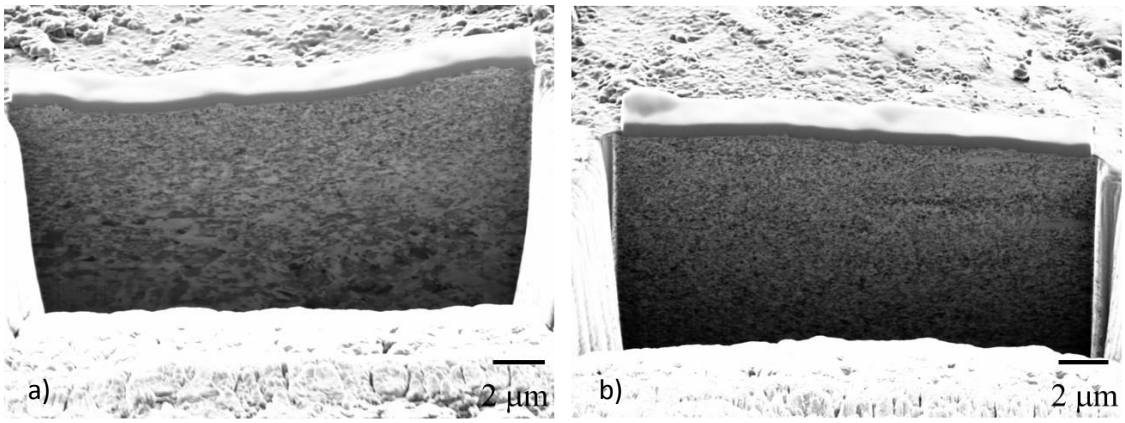

Figure 10. Analysis of the subsurface specimens by FIB/FESEM at the middel of the wear track: a) AR and b) 40CR.

Figure 11 shows a typical hardness profile measured in the specimens after wear tests. It sets the thickness of the hardened layer, defined as the distance from the surface to the zone where hardness reaches similar values to the bulk material. As it can be read in Table 2, the thicknesses of the hardened layer are higher for AR and 10CR conditions than for heavily cold rolled specimens, i.e. 20CR and 40CR. For the latter two cases, corresponding to specimens with greater amount of pre-existing martensite, the steel experienced lower plastic deformation, then promoting spalling and flaking phenomena. This involves a continuous removal of the surface material and, as a consequence, a reduction of the hardened layer thickness. This result is consistent with the larger wear volumes for 20CR and 40CR, that were reported in Figure 1.

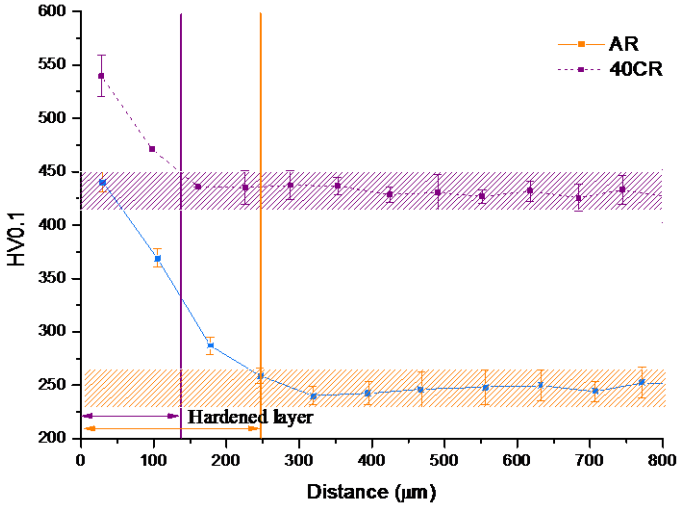

Figure 11. Hardness profiles for AR and 40CR specimens after 1000 m of sliding distance, where hardness of bulk material is represented as a colored strip. Each point is the average of four measurements.

Table 2. Thickness of the hardened layer for the four studied steel conditions after 100, 500 and 1000 m of sliding distance.

	Hardened layer (μm)		
	100 m	500 m	1000 m
AR	302±12	257±21	261±8
10CR	295±9	265±11	266±14
20CR	152±5	155±9	154±8
40CR	157±5	153±3	154±4

Hardness of cross-section achieved for all the studied steel conditions, as a function of the sliding distance, are plotted in Figure 12. Values follow a similar trend than the amount of martensite measured by XRD (see Fig. 3), i.e. a marked hardening is observed during the first 100 m of wear test, whereas a slight hardness increase takes place during the subsequent meters.

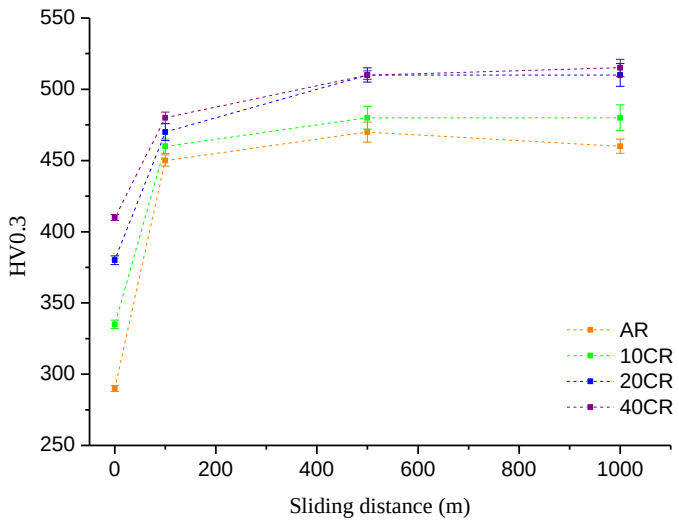

Figure 11. Hardness measured at the cross-sections of the studied steel conditions after wear tests from 100 to 1000 m.

Wear track morphology was analyzed by SEM. Similar wear mechanisms were observed in AR and CR specimens. After 100 meters of sliding distance, grooves in the sliding direction were the predominant feature (Fig. 12a), as a consequence of the local stress system associated with individual asperity contact characteristic of abrasive wear. At increasing sliding distances, plowing mechanism develops and becomes responsible of removing material by plowing the grooves in the form of ribbon-shaped debris particles, with part of them end up joining at the surface, as shown in Figure 12b.

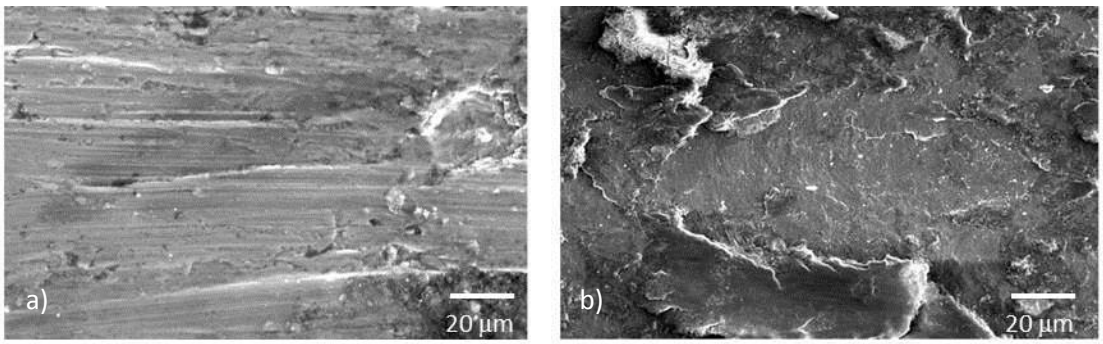

Figure 12. SEM micrograph of worn surfaces after: a) 100 m and b) 200m.

Evidences of oxidation in the wear track were observed for all the tested specimens. In this sense, figure 13 presents EDX maps where large areas of iron oxides are identifies. When increasing the sliding distances, a progressive growth of these oxidized regions was patent, as shown in Figures 14b to 14d. For test up to 100 to 300 m of sliding

distance, cracks at the oxide layer were observed (Fig. 14a), but later the accumulated damage on the track masked the evolution of this wear mechanism. . This phenomenon, known as tribocorrosion, lead to an irreversible transformation of the material resulting from the simultaneous physic-chemical and mechanical surface interactions occurring at a tribologic contact [44,45,46]. In passive materials, the origin of tribocorrosion is closely related to the presence of a protective oxide film of a few nanometers of thickness on the surfaces, mostly composed by oxides as a consequence of a spontaneous reaction [47,47]. .

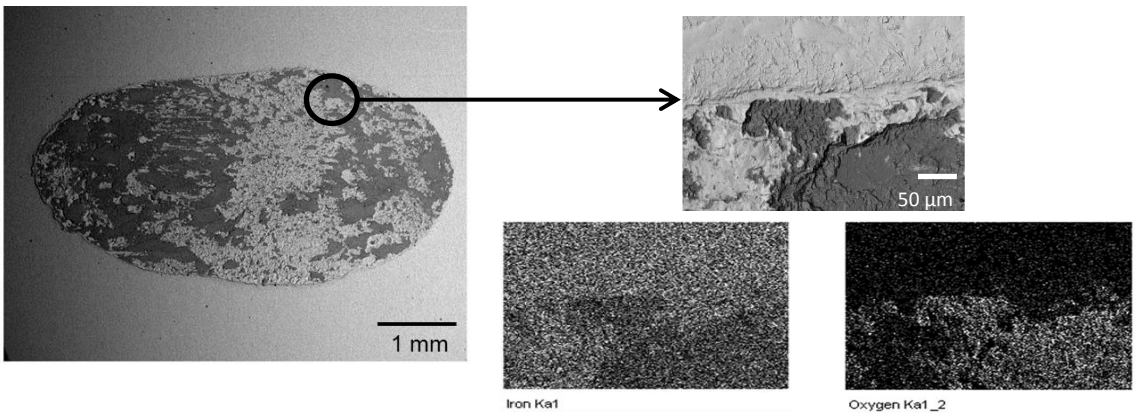

Figure 13. EDX mapping considering iron and oxygen of a tested specimen after 100m.

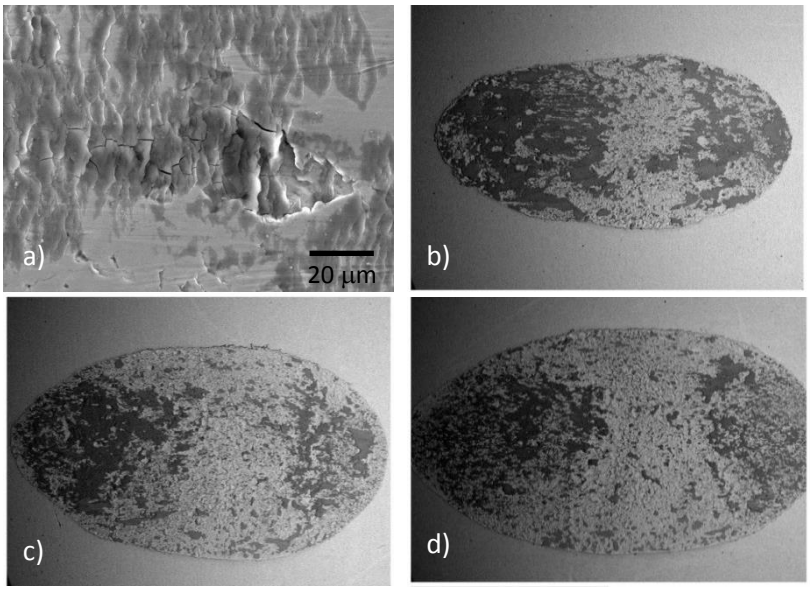

Figure 14. a) Magnification by SEM of a tested specimen after 200m, b-d) Appearance of the wear track after 100, 500 and 1000m respectively

4. Conclusions

Wear behavior of a metastable austenitic stainless steel was studied by considering four pre-existing martensite contents: less than 3% for the annealed condition, and between 9 and 38 % for cold rolled material. The main conclusions resulting from the investigation can be summarized as follows:

- Wear resistance was strongly influenced by the amount of pre-existing martensite. A direct correlation between wear rate and pre-existing martensite content was observed in the sliding tests. Therefore, annealed condition displayed the lowest wear rate.
- Wear tests promoted strain-induced martensite for all studied steel conditions. Moreover, the percentage of new martensite was higher for those conditions with greater amounts of pre-existing martensite. As a consequence, cold rolled specimens have a harder surface and plowing wear mechanism developed at lower degree compared to annealed conditions.
- A layer consisting of ultrafine-grains was observed just below the wear track regardless of the pre-existing martensite.
- Tribocorrosion was the main wear mechanism observed for all studied steel conditions. The formed oxide spreads all over the wear track as increasing sliding distances.

Acknowledgements

This work was carried out within the scope of MAT12-34602 project, supported by the Spanish Ministry of Economy and Competitiveness. We are grateful to "*Direcció General de Recerca del Comissionat per a Universitats i Recerca de la Generalitat de Catalunya*" for acknowledging CIEFMA as a consolidated Research group (2014SGR). Dr. J.J. Roa would like to thanks Juan de la Cierva Programme (grant number JCI-2012-14454) for its financial support.

References

[1] F. Placidi, F. Fraschetti: Potential application of stainless steel for vehicle crashworthiness structures. Technical report, Cenro sviluppo materiali, Italy.

[2] J.B. Vogt, Z. Magnin, J. Foct, Fatigue Fract.Eng.Mater.Struct.16 (1993) 555–564.

[3] R. Andersson, C. Magnusson, E. Schedin., Proc.Conf.of the Second Global Symposium on Innovations in Materials Processing and Manufacturing: Sheet Materials, 2001, TMS, NewOrleans, February11–15.ISBN0-87339-490-9.

[4] H.F.G. de Abreu, S.S. de Carvalho, P.L. Neto, R.P. dosSantos,V.N. Freire, P.M.O. Silva, S.S.M. Tavares, Mater.Res. 10(4) (2007) 359–366.

[5] P.L. Mangonon, G. Thomas, Metall.Trans. 1(6) (1970) 1577-1586.

[6] V. Seetharaman,P. Krishman, J.Mater.Sci., 16(2) (1981) 523–530.

[7] G. Nolze, Z. Metallkd. 95(9) (2004) 744–755.

[8] I. Gutierrez-Urrutia, D. Raabe, ActaMater. 59 (2011) 6449–6462.

[9] A. Prakash, T. Hochrainer, E. Reisacher, H. Riedel, Steel Res.Int. 79 (2008) 645–652.

[10] T. Niendorf, C. Lotze, D. Canadinc, A. Frehn, H.J. Maier, Mater, Mater.Sci.Eng. A 499 (2009) 518–524.

[11] A.S. Hamada, L.P .Karjalainen, J.Puustinen, Mater.Sci.Eng. A 517 (2009) 68–77.

[12] G. Frommeyer,U. Brux,P. Neuman, ISIJInt. 43 (2003) 438–446.

[13] Y.X. Wu,D. Tang, H.T .Jiang, Z.L. Mi, Y. Xue, H.P. Wu, J. Iron Steel Res. 21 (2004) 352–358.

[14] T.S. Byun: Acta Mater.,51(11) (2003) 3063-3071.

[15] J. Talonen, P. Nenonen, G. Pape, H. Hanninen, Met. Mat. Trans. A 36(2) (2005) 421-432.

[16] A.M. Beese, D. Mohr J. Mech. Phy. Sol. 60(11) (2012) 1922-1940.

[17] P.L. Mangonon, G. Thomas, Metall.Trans. 1(6) (1970) 1587-1594.

[18] I. Tamura, Metal Sci.16 (5) (1982) 245-253.

[19] K. Spencer, J.D. Embury, K.T. Conlon, M. Véron, Y. Bréchet, Mat. Sci. Eng. A 387-389 (2004) 873-881.

[20] G. Fargas, A. Zapata, J.J. Roa, I. Sapezanskaia, A. Mateo, Met. Mat. Trans. 46A (2015) 5697-5707.

[21] J. Stolarz, N. Baffie, T. Magnin, Mat. Sci. Eng. A, 319-321 (2001) 521-526.

[22] M. Topic, R.B. Tait , C. Allen, Int. J. Fatigue 29 (2007) 656-665.

[23] G. Fargas, A. Zapata, M. Anglada, A. Mateo, IOP Conf. Series: Materials Science and Engineering 5, 012008, 2009. ¿podemos referir a algún otro nuestro que esté en una revista buena?

[24] D. Mohan Lal, S. Renganarayanan, A.Kalanidhi, Cryogenics 4 (2001) 149-155.

[25] D. Das, K.K. Ray, A.K. Dutta, Mater. Sci. Eng. A 527 (2010) 2182-2193.

[26] K.L. Hsu, T.M. Ahn, D.A. Rugney, Wear 60 (1980) 13-67.

[27] Z.Y. Yang, M.G.S. Naylor, D.A. Rigney, Wear 105 (1985) 73-86.

[28] M.C-M. Farias, R.M. Souza, A. Sinatora, D.K. Tanaka, Wear 263 (2007) 773-781.

[29] Y-S Kim, S-D. Kim, S-J. Kim, Mat. Sci. Eng A 449-451 (2007) 1075-1078.

[30] M. Hua, X. Wei, J.Li, Wear 265 (2008)799-810.

[31] ASTM G99-04 Standard Test Method for Wear Testing with a Pin-on-Disk Apparatus, ASTM International, 2004.

[32] ASTM E975-03. Standard Practice for X-Ray Determination of Retained Austenite in Steel with Near Random Crystallographic Orientation. ASTM Internacional, 2003.REPETIDO

[33] I. Shakhovaa, V. Dudkoa, A. Belyakova, K. Tsuzakib, R. Kaibysheva, Mat.Sci.Eng.A 545 (2012) 176– 186.

[34] N. Nakada, H. Ito, Y. Matsuoka, T. Tsuchiyama, S. Takaki, Acta Mater. 58 (2010) 895–903.

[35] J.J. Roa, J.M.Wheeler, T.Trifonov, G.Fargas, A.Mateo, J.Michler, E. Jiménez-Piqué, Mat. Sci. Eng.A, 647 (2015), pp.51–57.

[36] Y. Tomota, H. Tokuda, Y. Adachi, M. Wakita, N. Minakawa, A. Moriai, Y. Morii, Acta Mater., 2004, 52 (20), pp. 5737-5745.

[37] J.N. Petch, J. Iron Steel Inst. 174 (1953) 25-28.

[38] E.O. Hall, Prco. Phys. Soc. 64B (1951) 747-753.

[39] G.R. Chanani, S.D. Antolovich, W.W. Gerberich: Metall. Trans. 3 (1972) 2661-2672.

[40] J.A. Muñoz, E. Jiménez-Piqué,J. Reyes, M. Anglada, Acta Mater.5 9(17) (2011) 6670–6683.

[41] A.P. Zhilyaev, J. Gubicza, G. Nurislamova, A. Révész, S. Surinach, M.D. Baro, Phys.Status Solidi A 198 (2003) 263–271.

[42] T. Ungar, G. Tichy, J. Gubicza, R.J. Hellmig,Powder Diffr. 20(2005) 366–375.

[43] P.V. Liddicoat, X.Z. Liao, Y. Zhao, Y. Zhu, M.Y. Murashkin, E.J. Lavernia, Nat. Commun. 1(2010)63–69.

[44] D. Landolt, S. Mischler, M. Stemp, S. Barril, Wear 256 (2004) 517–524.

[45] P. Jemmely, S. Mischler, D. Landolt, Wear 237 (2000) 63–76.

[46] N. Diomidis, J.-P. Celis, P. Ponthiaux, F.Wenger, Lubr.Sci. 21 (2009) 53–67.

[47] S. Mischler, A. Spiegel,D. Landolt, Wear 225–229 (1999) 1078–1087.

Suggested Reviewers

- Dr Andrew J Gant
National Physical Laboratory, Teddington,
andrew.gant@npl.co.uk

- Dr. Alejandro Sanz
IT Director of SKF Group
Alejandro.Sanz@skf.com

- Mirco D. Chapetti, Prof Eng PhD
Laboratory of Experimental Mechanics (LABMEX)
INTEMA - Research Institute for Materials Science
Department of Mechanical Engineering
CONICET - University of Mar del Plata
mchapetti@fi.mdp.edu.ar